OpenAccess

ORIGINAL PAPER

Video monitoring of neovessel occlusion induced by photodynamic therapy with verteporfin (Visudyne®), in the CAM model

E. Debefve · B. Pegaz · H. van den Bergh · G. Wagnières · N. Lange · J.-P. Ballini

Abstract The aim of the present study was to monitor photodynamic angioocclusion with verteporfin in capillaries. Details of this process were recorded under a microscope in real-time using a high-sensitivity video camera. A procedure was developed based on intravenous (i.v.) injection of a light-activated drug, Visudyne®, into the chorioallantoic membrane (CAM) of a 12-day-old chicken embryo. The effect of light activation was probed after 24 h by i.v. injection of a fluorescent dye (FITC dextran), and analysis of its fluorescence distribution. The angioocclusive effect was graded based on the size of the occluded vessels, and these results were compared with clinical observations. The time-resolved thrombus formation taking place in a fraction of the field of view was video recorded using a Peltier-cooled CCD camera. This vessel occlusion in the CAM model was reproducible and, in many ways, similar to that observed in the clinical use of verteporfin. The real-time video recording permitted the monitoring of platelet aggregation and revealed size-selective vascular closure as well as some degree of vasoconstriction. Platelets accumulated at intravascular junctions within seconds after verteporfin light activation, and capillaries were found to be closed 15 min later at the applied conditions. Larger-diameter vessels remained patent. Repetition of these data with a much more sensitive camera revealed occlusion of the treated area after 5 min with doses of verteporfin and light similar to those used clinically. Consequently, newly developed light-activated drugs can now be studied under clinically relevant conditions.

Introduction

Subfoveal choroidal neovascularization (CNV) is a degenerative condition that can cause severe, irreversible loss of central vision when unidentified and untreated. CNV can develop secondary to several disorders of the eye, including age-related macular degeneration (AMD), pathologic myopia, and ocular histoplasmosis syndrome [1]. AMD is the leading cause of blindness in people over 50 years of age in the Western world [2].

Thermal laser photocoagulation, as a treatment for CNV associated with AMD, can induce marked visual loss, and damage to the retinal pigment epithelium (RPE) and the neural retina [3]. The angioocclusive mechanism of action (MoA) of verteporfin (Visudyne®, Novartis Pharma AG, Basel, Switzerland) photodynamic therapy (PDT) represents one treatment option. The efficacy of verteporfin PDT has been investigated in more than 1,000 patients in Phase III trials. The first of these were the 'Treatment of Age-related Macular Degeneration with Photodynamic Therapy' (TAP) and Phase IIIb 'Verteporfin in Photodynamic Therapy' (VIP) studies [4, 5]. The benefits of verteporfin therapy on visual acuity were evident as early as 3 months after initial treatment, and were sustained throughout the 1- to 2-year follow-up periods, and eventually up to 6 years [4–7]. Verteporfin PDT is a minimally invasive, two-step

E. Debefve · B. Pegaz · H. van den Bergh (✉) · G. Wagnières ·
N. Lange · J.-P.Ballini
Ecole Polytechnique Fédérale de Lausanne, EPFL-ENAC-LPAS,
1015 Lausanne, Switzerland
e-mail: Hubert.vandenBergh@epfl.ch

process based on the interaction of verteporfin—an intravenously administered, non-toxic light-activated drug—with molecular oxygen. This interaction occurs after light is applied at an appropriate wavelength to the CNV lesion in the macula, where the verteporfin has accumulated to some extent preferentially [8], using a non-thermal diode laser device. The initial reaction of the light-activated drug with molecular oxygen leads to, among others, a short-lived reactive singlet oxygen intermediate, which reacts with the surrounding biomolecules and activates a cascade of chemical and physiological responses in the endothelial cells, which result in occlusion of the treated neovascularization [9]. Verteporfin (also known as benzoporphyrin-derivative monoacid ring A [BPD-MA]) is the active chemical component of the liposomal verteporfin formulation (Visudyne®), and is a potent, second-generation, light-activated drug derived from hematoporphyrin [10]. Animal studies have shown that the liposomal formulation of verteporfin accumulates selectively in the neovasculature by forming complexes with low-density lipoproteins (LDLs) [11, 12]. A clinical pharmacokinetic study further demonstrated that the retinal vessels are drained faster than the choroidal vessels, thus providing a time window of selectivity that helps, at least to some extent, to preserve the precious retinal capillaries [13–16]. The latter are probably also protected to some extent by the blood–retinal barrier. Most photosensitizers used in PDT induce vascular effects during and/or after light exposure of the tissue containing the photosensitizer. The mechanisms by which PDT induces haemostasis have been investigated in some detail. The main target of vascular PDT appears to be the endothelial cell [17–19]. The injected photosensitizer arrives at the endothelial cells and is partially internalized. Measuring the intracellular distribution of photosensitizing porphyrins has shown that, depending on the physico-chemical properties of the porphyrin, its fluorescence can be localized in the plasma membrane, cytoplasm, nuclear membrane, and nucleoli [20]. Light application causes the above-mentioned oxygen-radical-mediated damage to the cytoskeleton and other targets. Thus, PDT causes rounding and contraction of endothelial cells [9]. This results in the rupture of interendothelial cell tight junctions, thus exposing the subendothelial basement membrane (Fig. 1). PDT induces the release of von Willebrand factor [21], thromboxane, prostacyclin and other factors, such as vascular endothelial growth factor (VEGF), that result in increased vascular permeability and exudation, as well as clotting and vasoconstriction [17, 18, 22]. At the gaps formed between the rounded endothelial cells, activated platelets adhere to the damaged vessel wall. Platelets continue to aggregate and start to plug the vessel, finally leading to the formation of a fibrin-stabilized thrombus and vasoconstriction [23]. The ultimate outcome is haemostasis

with tissue hypoxia. Complete occlusion of the choroidal neovasculature can occur within 1 day. PDT can close smaller vessels more easily than larger vessels, as has been observed in the human choroid. Generally, the diameter of a vessel that can be occluded depends on the amount and location of the photosensitizer and on the light administered. Larger-diameter vessels, in which stasis has been observed, may re-open so that perfusion can be re-established.

The angiooocclusive properties of verteporfin therapy may close the CNV, sparing to a large extent the overlying retinal tissues; however, some degree of closure of the choriocapillaries is also observed [24]. At present, this unique MoA of verteporfin is still being investigated and, over the years, there have been considerable efforts to improve and develop instrumentation for clinical fluorescence diagnosis and PDT. Recent advances in understanding the multi-component pathogenesis of AMD, and the role of VEGF in CNV progression, have led to the development of antiangiogenic therapies. The latter include injection of the anti-VEGF agent ranibizumab (Lucentis®) [25]. Intravitreal ranibizumab had clinically been shown to safely prevent vision loss. It also improved mean visual acuity, over a 2-year period, in patients with minimally classic or occult CNV due to AMD [26]. Due to the promise of combining verteporfin with anti-VEGF and/or anti-inflammatory therapies, there is great interest in discovering and developing increasingly more selective photosensitizers to be used in the treatment of CNV due to AMD. Consequently, efficient in vivo drug screening procedures that help define vascular PDT effects are vital in the development of new photosensitive drugs and optimizing the experimental conditions. An extensive intercomparison of photosensitizers for PDT closure of CNV associated with AMD has been initiated using an in vivo model optimized for vascular thrombosis studies [27].

The chorioallantoic membrane (CAM) of the chicken embryo has been used as an in vivo assay for PDT and as a model for studying biological processes related to high angiogenic activity. In this model, the vessels are of the neovessel type and are representative of neovascular growth due to the embryonic phase of the egg; thus, the events occurring at the cellular level can be, at least to some extent, linked to those occurring at the endothelial cell level of the CNV neovessels in the eye. This approach allows for concurrent observation of the activity of different photosensitizers, as well as direct visualization of blood vessels before, during, and after PDT. The CAM is a major respiratory organ of the chicken embryo, and the well-vascularized surface is formed through fusion of two mesodermal layers. It is relatively inexpensive, easily accessible, and has a high transparency that allows nearly any wavelength in the visible and near infrared parts of the
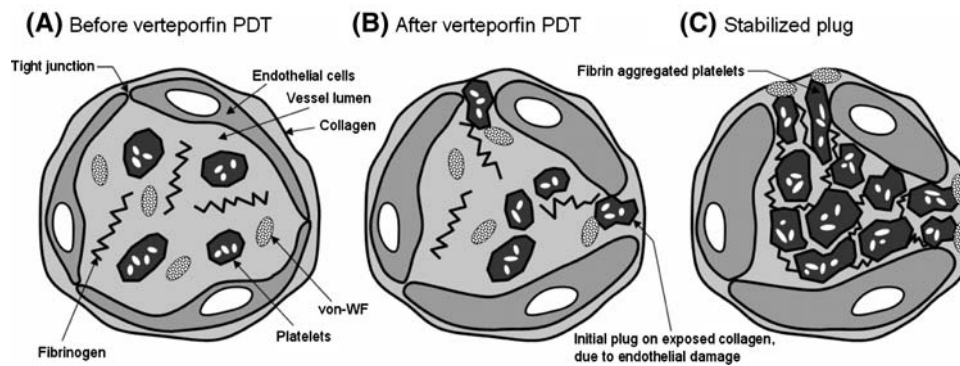
Fig. 1 A simplified sequence describing verteporfin PDT-induced changes to the endothelium. (**a**) Blood vessel wall before verteporfin PDT; endothelial cells lining the vessel wall are bound by tight junctions. (**b**) Verteporfin PDT-induced oxidative stress to the endothelium alters the cytoskeleton and triggers rounding and retraction of endothelial cells, consequently exposing subendothelial connective tissue; von Willebrand (von-WF) and other clotting factors are released at the exposed site, and platelets adhere to the damaged surface. (**c**) Finally, a stabilized fibrin plug is formed as the blood clots

electromagnetic spectrum to be used in dye excitation and fluorescence analyses, making it ideal as a model for directly observing the vascular effects of PDT.

The aim of this study was to monitor the mechanisms of angioocclusion with verteporfin PDT at the capillary vessels level and to record events in real-time, using a high-sensitivity video camera.

Methods

An experimental procedure was developed using intravenous (i.v.) injection of various photosensitizers and fluorescent dyes into the CAM for drug screening and prediction of clinical features.

CAM preparation

Fertilized chicken eggs were disinfected, numbered, and transferred into a turning incubator, set at 37°C and 60% humidity [27]. On embryo development day (EDD) 3, a hole of approximately 3 mm in diameter was drilled into each eggshell and covered with cling film. The eggs were then returned to the incubator in a static position until use at approximately EDD 12 [27]. The correlation in PDT vessel closure efficiency between the model and CNV in human eyes was established using both verteporfin and lutetium texaphyrin (Lutex®), because data were available on both substances from both CAM and human clinical trials. The angiographic dyes indocyanine green and fluorescein were also tested in both model and clinical context.

Measuring angioocclusion

On EDD 13, the holes were extended to a diameter of approximately 30 mm, and the embryos were placed under an epi-fluorescence microscope (Nikon Eclipse E600 FN, Japan) equipped with long-working-distance Nikon objectives (CFI $4\times/0.10$, WD $= 30$; PlanFluor $10\times/0.30$, WD $= 16$; L-Plan SLWD $20\times/0.35$, WD $= 24$; or L-Plan SLWD $50\times/0.45$, WD $= 17$) and with an F-view II 12-bit monochrome Peltier-cooled digital CCD camera driven with analySIS® docu software from Soft Imaging System (Münster, Germany).

Verteporfin was intravenously injected into the vasculature of the fertilized chicken eggs. The development of thrombosis was recorded during and after light activation in real-time using the described digital CCD camera or an ultra-high-sensitivity video camera (EM-CCD, Hamamatsu, Japan) (Fig. 2). This on-chip amplified Hamamatsu electron multiplier, back-thinned, Peltier-cooled CCD camera (EM-CCD C9100-12; 400–1,000 nm) provided up to $2,000\times$ signal amplifier gain, thus allowing a lower level of excitation light to be used. This level of excitation corresponds closely to that used in the human eye. Images and sequences were recorded through the Hamamatsu
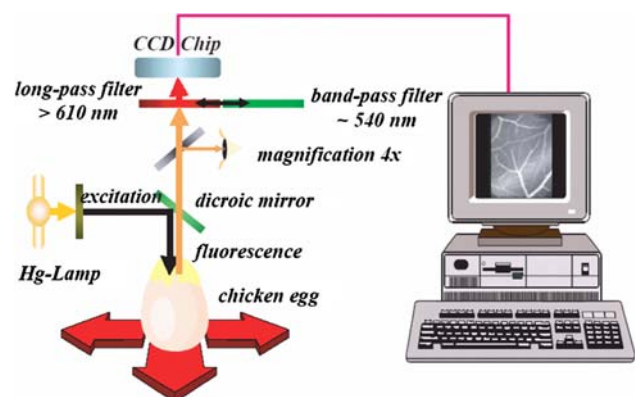

Fig. 2 Experimental set-up. Excitation was performed at 420 nm for verteporfin activation and 470 nm for FTIC fluorescence recording

camera controller with the Hamamatsu HiPic version 7.0 software, giving 512×512 pixels, 16-bit grey-level images. Selective angiooclusion, as controlled mainly by the optical field of exposure (diaphragm), was observed in the CAM chicken embryo model, following verteporfin therapy. This was done by visualizing the location and aggregation of platelets on video recordings. Images were recorded at 12 frames per second.

Results

Standard-sensitivity camera

Vessel occlusion, similar to that in clinical PDT, was reproducible in the CAM model. Total photothrombosis of treated vessels was observed at a photosensitizer dose of 0.15 mg/kg and 60 J/cm^2 of 689 nm light in the human eye, and 0.4 mg/kg photosensitizer and 25 J/cm^2 at 420 nm in the CAM model (Fig. 3). Standard doses in humans are 6 mg/m^2 body surface area, approximately 0.15 mg/kg body weight, and 50 J/cm^2 of 689 nm light applied for 83 s at an intensity of 600 mW/cm^2, 15 min after the start of injection, which lasted for ~ 10 min. Standard doses for the CAM were 0.2 mg/kg body weight of embryo (~ 10 g) [28], and 20 J/cm^2 of a filtered Hg-arc lamp at 420 ± 20 nm light for a duration of ~ 60 s at a fluence of 330 mW/cm^2. This technique allowed a real-time view of verteporfin-induced angiooclusive events in the CAM of a gestating chicken egg.

The video recording permitted monitoring of the location and speed of adhesion, aggregation and release of platelets, and showed an end result of selective vascular closure (Fig. 4). Platelets built up at intracellular junctions seconds after the activation of verteporfin. Formation of a stabilized plug leading to complete closure of a capillary was observed 15 min after verteporfin activation, while bloodflow continued in the much larger-diameter main vessel (Fig. 4). Because a relatively high magnification ($50\times$) was used to optimize the observation of angiooclusion at the capillary vessels level, the observed area

received a higher fluence rate (≥ 1 W/cm^2) compared with the clinical situation (600 mW/cm^2).

Ultra-high-sensitivity camera

With this magnification ($50\times$), to record angiooclusion under conditions that were close to the clinical setting, the excitation light had to be lowered by two orders of magnitude to maintain a fluence level much lower than 330 mW/cm^2 on the CAM surface, and thus did not cause PDT while recording video images. Therefore, the sensitivity of the recording device (EM-CCD) was increased proportionately to record images at the lower illumination. The ultra-high-sensitivity camera permitted monitoring of angiooclusion using verteporfin PDT with light and drug doses similar to those utilized in the human clinical setting (Fig. 5). Following a co-injection of verteporfin and FITC dextran, light was applied to the treated area for 1 min at a wavelength of 420 nm, followed by administration of a non-therapeutic wavelength (470 nm) (verteporfin absorbance 1/3) attenuated to 1/30 (~ 10 mW/cm^2) to record the flow of blood within the vessels (FITC dextran fluorescence), using two different magnifications (Nikon $10\times$, $50\times$) (Fig. 5). Thus, the resultant excitation was reduced to $\sim 1\%$ of the original excitation. Occlusion of the treated area was observed after 5 min of light exposure at a wavelength of 420 nm (Fig. 5b–f for $10\times$, and Fig. 5g–j for $50\times$ magnification).

The effect of light dose and drug concentration on the level of angiooclusion with verteporfin was also investigated in the CAM model, using a 6-point scale from 0 (no occlusion) to 5 (total occlusion in treated area) (Table 1). Twenty-four hours after treatment, a dose-proportional increase in the level of vascular occlusion was observed with increasing fluence (from 10 to 40 J/cm^2) and drug concentration (from 100 to 200 µg/kg), (Fig. 6a–g).

Discussion

Verteporfin PDT has provided significant improvements in the management of subfoveal CNV for hundreds of

Fig. 3 Photosensitizer efficacy. Reproduced with permission from Ref. [8]

Human Visudyne
0.15 mg/kg, 60 J/cm^2
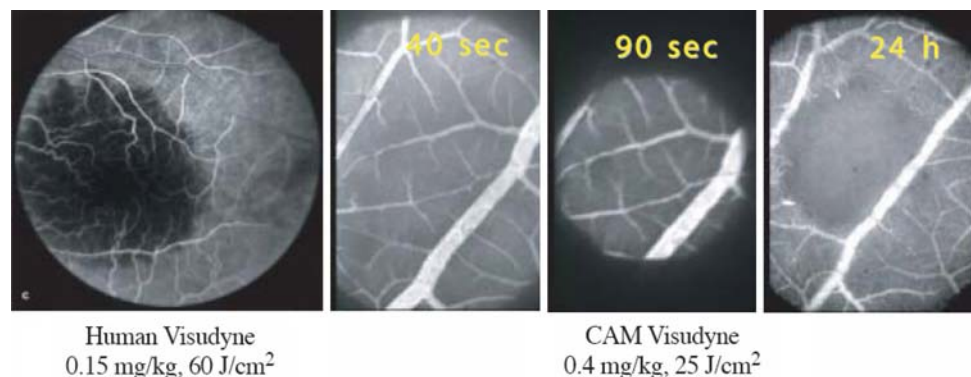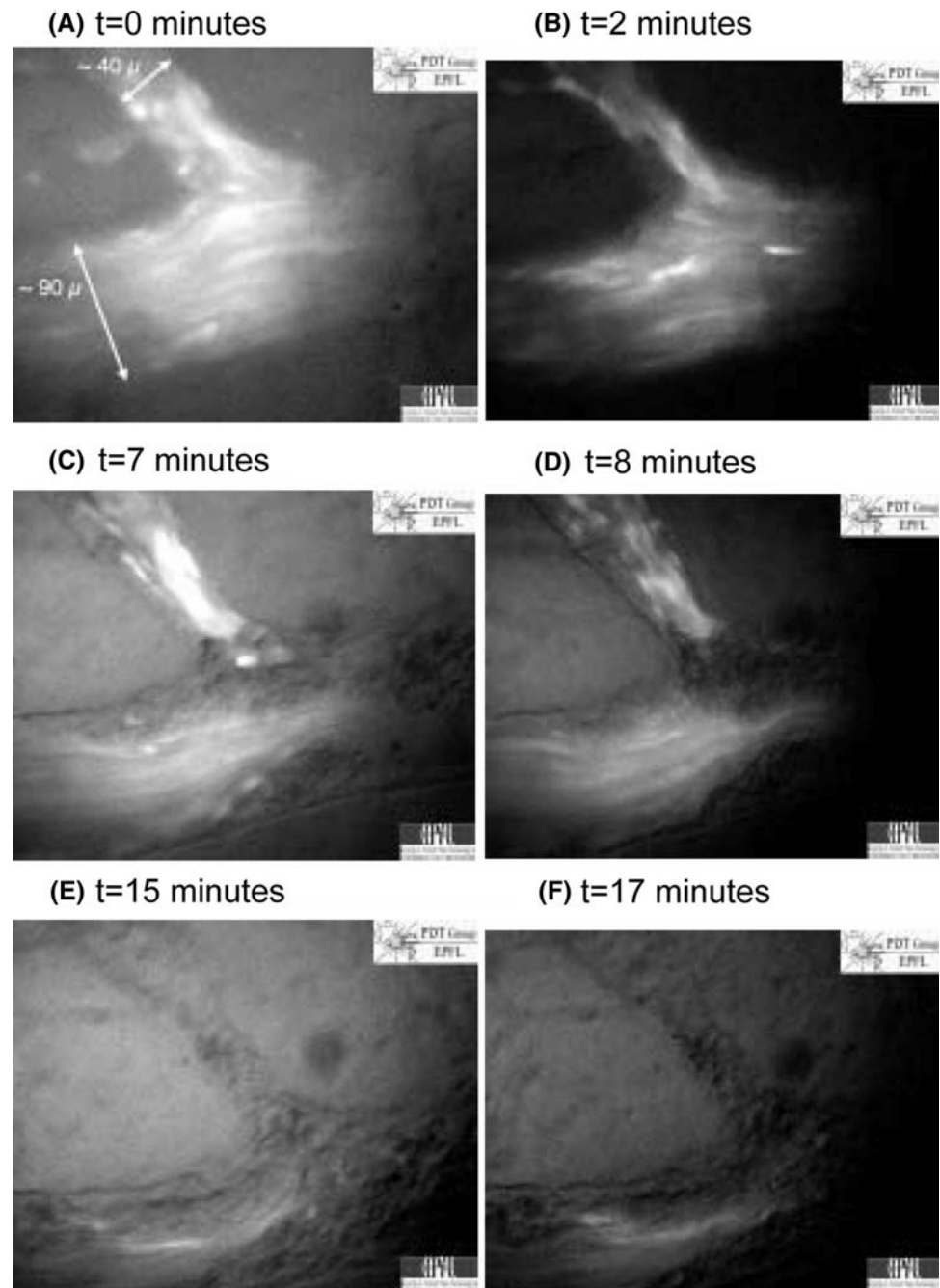
CAM Visudyne
0.4 mg/kg, 25 J/cm^2

Fig. 4 Images from illumination of the CAM model showing formation of a stabilized plug, leading to complete closure of the capillary 15 min after verteporfin activation. Image dimensions = 280 × 224 μm

(A) t=0 minutes

(B) t=2 minutes

(C) t=7 minutes

(D) t=8 minutes

(E) t=15 minutes

(F) t=17 minutes

thousands of patients. The long-term proven stability in vision often provides additional low-vision rehabilitation [29, 30], and also a gain in contrast sensitivity, compared with placebo [31, 32]. PDT has a potential dual selectivity, because there is a preferential accumulation of verteporfin in the target tissue, and light application is confined to the specific target area [24]. Furthermore, the retinal vasculature is protected by the blood–retinal barrier. Selectively destroying the abnormal new choroidal vessels while sparing normal vessels in the retina and choroid is crucial for maintaining neural retina function in CNV therapy. The

selectivity of verteporfin was first demonstrated in animal models, in which photodynamic damage was spatially confined to vascular structures [12, 33, 34]. In vivo studies in the rabbit cornea showed that verteporfin was rapidly and selectively taken up by neovascular endothelium and caused a complete and selective occlusion without alteration of the adjacent stroma [35]. Further studies showed that verteporfin therapy selectively occluded the subretinal choriocapillary layer while sparing the sensitive overlying retinal structures [33]. In monkeys, verteporfin selectively occluded CNV, while sparing retinal vessels and large,
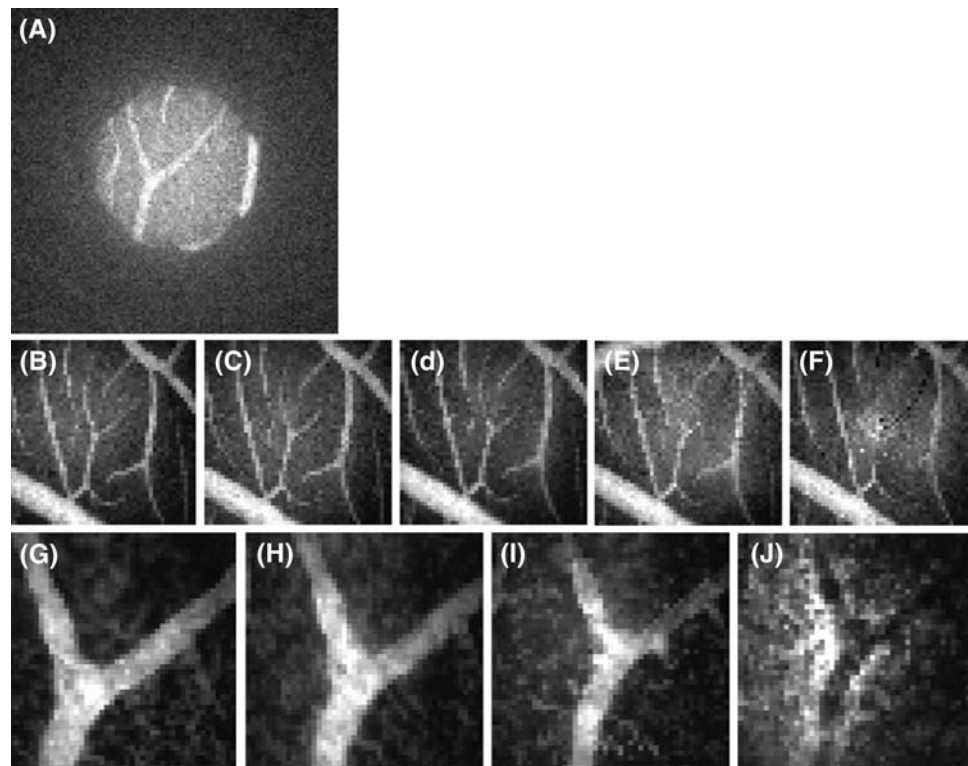
Table 1 Scale of verteporfin PDT-induced angioocclusion in vessels of the CAM model [27]

| Scale of angioocclusion efficacy*	Criterion
0	No occlusion
1	Partial closure of capillaries of diameter <10 μm
2	Closure of capillary system, partial closure of blood vessels of diameter <30 μm and size reduction of larger blood vessels
3	Closure of vessels of diameter <30 μm and partial closure of higher order vessels
4	Total closure of vessels of diameter <70 μm and partial closure of larger vessels
5	Total occlusion of vessels in the treated area

* Intermediate values are found when making the average of different scores

normal choroidal vessels [15, 36]. Overall, preclinical studies demonstrated that, although verteporfin therapy may cause some reversible damage to the RPE and outer retina, only minimal damage was observed in normal intraocular tissues such as retinal vessels, underlying choroid, and overlying neurosensory retina [12, 15, 36–38]. These data suggested that verteporfin could be a useful tool to treat selectively subretinal neovascularization, such as CNV in AMD. The aim of verteporfin therapy is to selectively occlude or destroy CNV, while sparing perfusion in the deeper, larger choroidal vessels and overlying retinal tissue and retinal vessels. A dose-ranging study showed that the minimally effective and maximally tolerated light doses were ≥ 25 J/cm^2 and significantly less than 150 J/cm^2, respectively [39, 40]. At a light dose equal to or above 150 J/cm^2, non-perfusion of neurosensory retinal vessels was observed leading to blindness spots in those eyes [40]. The optimal dose was determined to be a 10-min i.v. infusion of 6 mg/m^2 (0.15 mg/kg for a 2 m^2, 80 kg human) verteporfin, and a light dose of 50 J/cm^2 delivered over a period of approximately 83 s. The optimal time for irradiation (at 690 nm, light intensity 600 mW/cm^2) was 15 min after the start of verteporfin infusion. Although verteporfin therapy is generally considered to be a selective treatment [24, 41], there is some evidence of choroidal hypoperfusion following treatment with verteporfin monotherapy [42–44].

The CAM chicken embryo is a useful model with which to investigate Photofrin®-based PDT-induced vascular effects following topical application of a variety of photosensitizers, including verteporfin, sulfonated chloro-aluminum phthalocyanine (AlPcSn), and Lutex® [45], all of which were evaluated for their photothrombotic efficacy. A considerable variation exists between the different photosensitizers in terms of biophysical and biochemical characteristics, biodistribution and uptake kinetics, as well as in terms of the vehicle and/or formulation used [46–50].

Fig. 6 Dose-proportional effect of increasing light dose and drug concentration on vascular occlusion efficacy of verteporfin in the CAM model
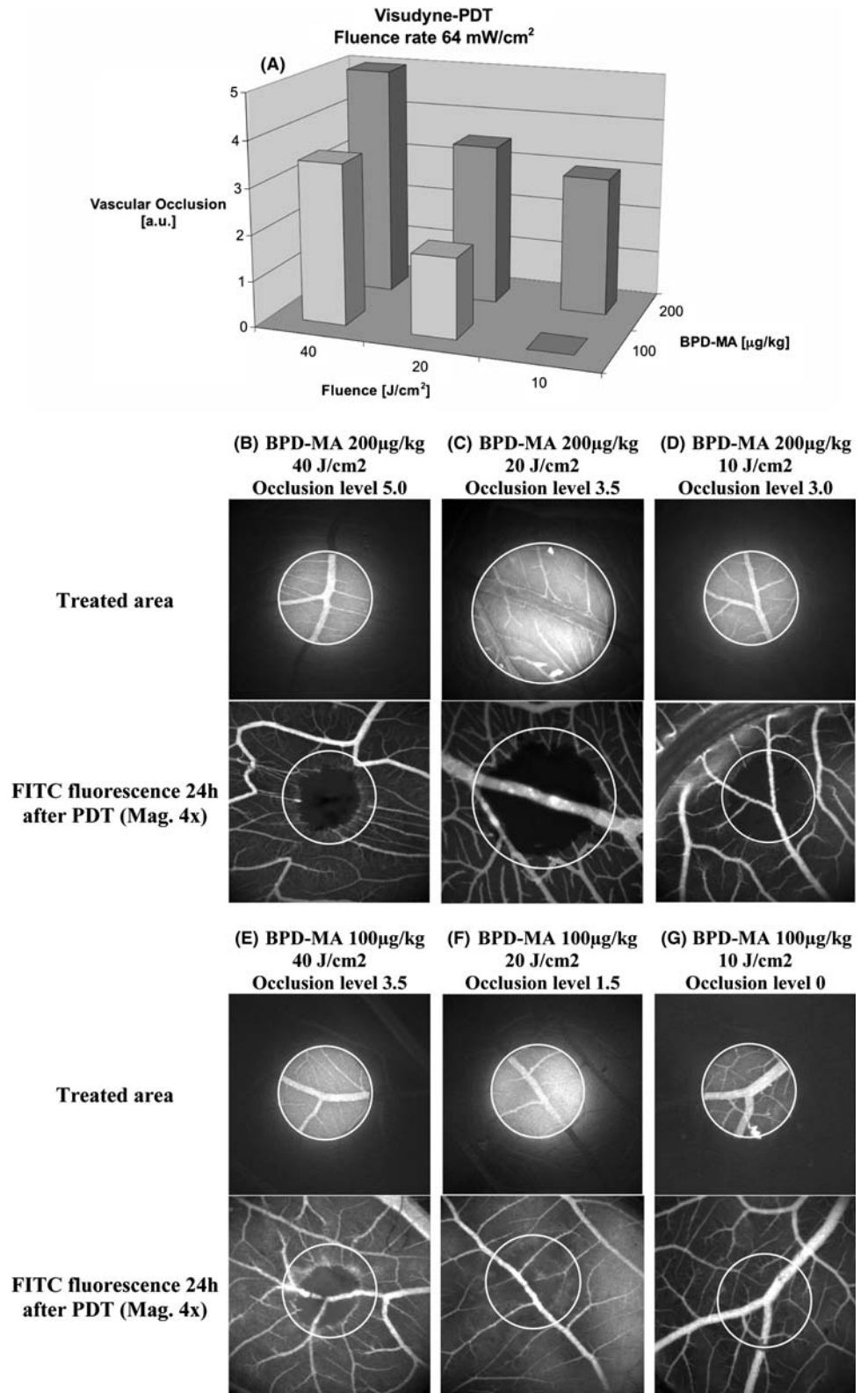
The present study reports that real-time video recording of verteporfin-induced neovessel thrombosis using the CAM model and a standard-sensitivity camera allowed monitoring of the location, aggregation and release of platelets, with an end result of selective vascular closure after 5–15 min. Some aspects of the dose-proportionality and selectivity of verteporfin therapy were demonstrated in the CAM chicken embryo model. Importantly, the size

selectivity of verteporfin for the closure of smaller vessels was demonstrated in this model—the images show stasis in the smaller vessels while blood continued to flow in the larger-diameter vessels. The effects observed after low-light fluorescence activation of verteporfin showed strong similarities of the structural effects to those observed in the human eye during clinical trials. However, there was an inherent experimental problem, due to the use of a much higher magnification ($50\times$) with this apparatus, which was needed to observe more closely the events occurring at the capillary level. Due to the recording of images during the process of photothrombosis, the area under investigation received a much higher level of illumination intensity than in the clinical situation. A more appropriate verteporfin therapy light level, i.e. close to the clinical context, was achieved by reducing the illumination intensity and changing the wavelength to one that was absorbed less, which together reduced the excitation to $\sim 1\%$ of the previously used levels. In addition, an ultra-high-sensitivity video camera was used to record the data. The ultra-high-sensitivity camera permitted monitoring of angiooclusion under conditions that did not induce more photodynamic activity while recording images.

The effects of verteporfin therapy on the vasculature are now being investigated using a nude-mouse dorsal skin-fold chamber model (at EPFL, CHUV Hospital, Lausanne, Switzerland). Adult nude mice receive i.v. injections of verteporfin, and the effects on the vasculature are visualized using intravital microscopy during and after light activation. The conditions again closely resemble those in the clinical setting, but because neovessels are not involved in the present experiments, higher verteporfin doses ($\times 4$) and light levels ($\times 4$) are being used.

With the increasingly widespread use of antiangiogenic agents, such as ranibizumab, for the treatment of CNV due to AMD, this model may also provide a useful tool with which to investigate the potential synergistic effects of combining angioocclusive verteporfin therapy with anti-VEGF agents. For example, this model would be useful to investigate whether anti-VEGF therapies sensitize vessels to verteporfin PDT or whether the angioocclusive effect persisted for a longer period of time in the presence of anti-VEGF agents. Moreover, this model will be instrumental in assessing the activity and selectivity of a new generation of photosensitizers, under a variety of experimental conditions, to be used in the treatment of CNV due to AMD.

References

1. Rubin GS, Roche KB, Prasada-Rao P, Fried LP (1994) Visual impairment and disability in older adults. Optom Vis Sci 71:750–760
2. Ciulla TA, Danis RP, Harris A (1998) Age-related macular degeneration: a review of experimental treatments. Surv Ophthalmol 43:134–146
3. Macular photocoagulation study group (1994) Visual outcome after laser photocoagulation for subfoveal choroidal neovascularization secondary to age-related macular degeneration. The influence of initial lesion size and initial visual acuity. Arch Ophthalmol 112:480–488
4. Treatment of age-related macular degeneration with photodynamic therapy (TAP) study group (1999) Photodynamic therapy of subfoveal choroidal neovascularization in age-related macular degeneration with verteporfin: one-year results of 2 randomized clinical trials-TAP Report 1. Arch Ophthalmol 117:1329–1345
5. Verteporfin in photodynamic therapy (VIP) study group (2001) Verteporfin therapy of subfoveal choroidal neovascularization in age-related macular degeneration: two-year results of a randomized clinical trial including lesions with occult with no classic choroidal neovascularization—verteporfin in photodynamic therapy report 2. Am J Ophthalmol 131:541–560
6. Treatment of age-related macular degeneration with photodynamic therapy (TAP) study group (2001) Photodynamic therapy of subfoveal choroidal neovascularization in age-related macular degeneration with verteporfin: two-year results of 2 randomized clinical trials—TAP report 2. Arch Ophthalmol 119:198–207
7. Verteporfin in photodynamic therapy (VIP) study group (2003) Verteporfin therapy of subfoveal choroidal neovascularization in pathologic myopia: 2-year results of a randomized clinical trial—VIP report no. 3. Ophthalmology 110:667–673
8. Van den Bergh H, Ballini J-P (2003) Photodynamic therapy: basic principles and mechanisms. In: Frankhauser F, Kwasniewska S (eds) Lasers in ophthalmology—basic, diagnostic and surgical aspects. A review. Kugler Publications, The Hague, The Netherland
9. Fingar VH (1996) Vascular effects of photodynamic therapy. J Clin Laser Med Surg 14:323–328
10. Mellish KJ, Brown SB (2001) Verteporfin: a milestone in opthalmology and photodynamic therapy. Expert Opin Pharmacother 2:351–361
11. Schmidt U, Birngruber R, Hasan T (1992) Selective occlusion of ocular neovascularization by photodynamic therapy. Ophthalmologe 89:391–394
12. Schmidt-Erfurth U, Hasan T, Gragoudas E et al (1994) Vascular targeting in photodynamic occlusion of subretinal vessels. Ophthalmology 101:1953–1961
13. Houle JM, Strong A (2002) Clinical pharmacokinetics of verteporfin. J Clin Pharmacol 42:547–557
14. Miller H, Miller B (1993) Photodynamic therapy of subretinal neovascularization in the monkey eye. Arch Ophthalmol 111:855–860
15. Miller JW, Walsh AW, Kramer M et al (1995) Photodynamic therapy of experimental choroidal neovascularization using lipoprotein-delivered benzoporphyrin. Arch Ophthalmol 113:810–818
16. Van den Bergh H, Ballini JP, Sickenberg M (2004) On the selectivity of photodynamic therapy of choroidal neovascularization associated with age-related macular degeneration. J Fr Ophtalmol 27:75–78
17. Ben Hur E, Heldman E, Crane SW, Rosenthal I (1988) Release of clotting factors from photosensitized endothelial cells: a possible trigger for blood vessel occlusion by photodynamic therapy. FEBS Lett 236:105–108

18. Schuster A, Oishi H, Beny JL, Stergiopulos N, Meister JJ (2001) Simultaneous arterial calcium dynamics and diameter measurements: application to myoendothelial communication. Am J Physiol Heart Circ Physiol 280:H1088–H1096

19. West CM, West DC, Kumar S, Moore JV (1990) A comparison of the sensitivity to photodynamic treatment of endothelial and tumour cells in different proliferative states. Int J Radiat Biol 58:145–156

20. Schneckenburger H, Ruck A, Bartos B, Steiner R (1988) Intracellular distribution of photosensitizing porphyrins measured by video-enhanced fluorescence microscopy. J Photochem Photobiol B 2:355–363

21. Foster TH, Primavera MC, Marder VJ, Hilf R, Sporn LA (1991) Photosensitized release of von Willebrand factor from cultured human endothelial cells. Cancer Res 51:3261–3266

22. Schmidt-Erfurth U, Schlotzer-Schrehard U, Cursiefen C et al (2003) Influence of photodynamic therapy on expression of vascular endothelial growth factor (VEGF), VEGF receptor 3, and pigment epithelium-derived factor. Invest Ophthalmol Vis Sci 44:4473–4480

23. Andre P, Denis CV, Ware J et al (2000) Platelets adhere to and translocate on von Willebrand factor presented by endothelium in stimulated veins. Blood 96:3322–3328

24. Schmidt-Erfurth U, Hasan T (2000) Mechanisms of action of photodynamic therapy with verteporfin for the treatment of age-related macular degeneration. Surv Ophthalmol 45:195–214

25. Augustin AJ, Offermann I (2006) Emerging drugs for age-related macular degeneration. Expert Opin Emerg Drugs 11:725–740

26. Rosenfeld PJ, Brown DM, Heier JS et al (2006) Ranibizumab for neovascular age-related macular degeneration. N Engl J Med 355:1419–1431

27. Lange N, Ballini JP, Wagnieres G, van den Bergh H (2001) A new drug-screening procedure for photosensitizing agents used in photodynamic therapy for CNV. Invest Ophthalmol Vis Sci 42:38–46

28. Romanoff AL (1967) Biochemistry of the avian embryo: a quantitative analysis of prenatal development. Interscience, New York

29. Kaiser PK (2006) Treatment of age-related macular degeneration with photodynamic therapy (TAP) study group. Verteporfin therapy of subfoveal choroidal neovascularization in age-related macular degeneration: 5-year results of two randomized clinical trials with an open-label extension—TAP report no. 8. Graefes Arch Clin Exp Ophthalmol 244:1132–1142

30. Sickenberg M, Ballini JP, van den Bergh H (2004) [Visudyne photodynamic therapy and feeder vessel occlusion: rationale of a synergistic association and clinical options]. J Fr Ophtalmol 27:93–102

31. Rubin GS, Bressler NM (2002) Effects of verteporfin therapy on contrast sensitivity: results from the treatment of age-related macular degeneration with photodynamic therapy (TAP) Investigation—TAP report no. 4. Retina 22:536–544

32. Mones J, Rubin GS (2005) Contrast sensitivity as an outcome measure in patients with subfoveal choroidal neovascularisation due to age-related macular degeneration. Eye 19:1142–1150

33. Schmidt-Erfurth U, Bauman W, Gragoudas E et al (1994) Photodynamic therapy of experimental choroidal melanoma using lipoprotein-delivered benzoporphyrin. Ophthalmology 101:89–99

34. Schmidt-Erfurth U, Flotte TJ, Gragoudas ES et al (1996) Benzoporphyrin–lipoprotein-mediated photodestruction of intraocular tumors. Exp Eye Res 62:1–10

35. Schmidt-Erfurth U, Hasan T, Schomacker K, Flotte T, Birngruber R (1995) In vivo uptake of liposomal benzoporphyrin derivative and photothrombosis in experimental corneal neovascularization. Lasers Surg Med 17:178–188

36. Kramer M, Miller JW, Michaud N et al (1996) Liposomal benzoporphyrin derivative verteporfin photodynamic therapy. Selective treatment of choroidal neovascularization in monkeys. Ophthalmology 103:427–438

37. Husain D, Miller JW, Michaud N et al (1996) Intravenous infusion of liposomal benzoporphyrin derivative for photodynamic therapy of experimental choroidal neovascularization. Arch Ophthalmol 114:978–985

38. Lin SC, Lin CP, Feld JR, Duker JS, Puliafito CA (1994) The photodynamic occlusion of choroidal vessels using benzoporphyrin derivative. Curr Eye Res 13:513–522

39. Schmidt-Erfurth U, Miller J, Sickenberg M et al (1998) Photodynamic therapy of subfoveal choroidal neovascularization: clinical and angiographic examples. Graefes Arch Clin Exp Ophthalmol 236:365–374

40. Miller JW, Schmidt-Erfurth U, Sickenberg M et al (1999) Photodynamic therapy with verteporfin for choroidal neovascularization caused by age-related macular degeneration: results of a single treatment in a phase 1 and 2 study. Arch Ophthalmol 117:1161–1173

41. Schlotzer-Schrehardt U, Viestenz A, Naumann GO et al (2002) Dose-related structural effects of photodynamic therapy on choroidal and retinal structures of human eyes. Graefes Arch Clin Exp Ophthalmol 240:748–757

42. Gelisken F, Lafaut BA, Inhoffen W et al (2004) Clinicopathological findings of choroidal neovascularisation following verteporfin photodynamic therapy. Br J Ophthalmol 88:207–211

43. Recchia FM, Greenbaum S, Recchia CA et al (2006) Self-reported acute decrease in visual acuity after photodynamic therapy for age-related macular degeneration. Retina 26:1042–1048

44. Cardillo PF, Eandi CM, Ventre L, Rigault de la Longrais RC, Grignolo FM (2003) Photodynamic therapy for chronic central serous chorioretinopathy. Retina 23:752–763

45. Hammer-Wilson MJ, Akian L, Espinoza J, Kimel S, Berns MW (1999) Photodynamic parameters in the chick chorioallantoic membrane (CAM) bioassay for topically applied photosensitizers. J Photochem Photobiol B 53:44–52

46. Vargas A, Pegaz B, Debefve E et al (2004) Improved photodynamic activity of porphyrin loaded into nanoparticles: an in vivo evaluation using chick embryos. Int J Pharm 286:131–145

47. Pegaz B, Debefve E, Borle F et al (2005) Encapsulation of porphyrins and chlorins in biodegradable nanoparticles: the effect of dye lipophilicity on the extravasation and the photothrombic activity. A comparative study. J Photochem Photobiol B 80:19–27

48. Pegaz B, Debefve E, Borle F et al (2005) Preclinical evaluation of a novel water-soluble chlorin E6 derivative (BLC 1010) as photosensitizer for the closure of the neovessels. Photochem Photobiol 81:1505–1510

49. Pegaz B, Debefve E, Ballini JP et al (2006) Photothrombic activity of m-THPC-loaded liposomal formulations: pre-clinical assessment on chick chorioallantoic membrane model. Eur J Pharm Sci 28:134–140

50. Pegaz B, Debefve E, Ballini JP, Konan-Kouakou YN, van den Bergh H (2006) Effect of nanoparticle size on the extravasation and the photothrombic activity of meso(p-tetracarboxyphenyl)porphyrin. J Photochem Photobiol B 85:216–222